Journal of Controlled Release 143 (2010) 112–119

Contents lists available at ScienceDirect

Journal of Controlled Release

journal homepage: www.elsevier.com/locate/jconrel

Polyplex nanomicelle promotes hydrodynamic gene introduction to skeletal muscle

Keiji Itaka [a,c], Kensuke Osada [b,c], Katsue Morii [a], Pilhan Kim [d], Seok-Hyun Yun [d], Kazunori Kataoka [a,b,c,*]

[a] Division of Clinical Biotechnology, Center for Disease Biology and Integrative Medicine, Graduate School of Medicine, The University of Tokyo, Japan
[b] Department of Materials Science and Engineering, Graduate School of Engineering, The University of Tokyo, Japan
[c] Center for Nanobio Integration, The University of Tokyo, 7-3-1 Hongo, Bunkyo-ku, Tokyo 113-0033, Japan
[d] Harvard Medical School and Wellman Center for Photomedicine, Massachusetts General Hospital, 50 Blossom Street, Boston, MA 02114, USA

ARTICLE INFO

Article history:
Received 15 September 2009
Accepted 16 December 2009
Available online 3 January 2010

Keywords:
Muscle gene delivery
Hydrodynamic delivery
Polyplex nanomicelle
Plasmid DNA
Intravenous injection

ABSTRACT

Skeletal muscle is an interesting target for gene therapy. To achieve effective gene introduction in skeletal muscle, a hydrodynamic approach by intravenous injection of plasmid DNA (pDNA) with transient isolation of the limb has attracted attention. In this study, we demonstrated that polyplex nanomicelle, composed of poly(ethyleneglycol) (PEG)-block-polycation and pDNA, showed excellent capacity of gene introduction to skeletal muscle. The evaluation of luciferase expression in the muscle revealed that the nanomicelle provided higher and sustained profiles of transgene expression compared with naked pDNA. Real-time *in vivo* imaging using a video-rate confocal imaging system suggested that the nanomicelle showed tolerability in the intracellular environment, resulting in the slow but sustained transgene expression. The nanomicelle induced less TNFα induction in the muscle than naked pDNA, indicating the safety of nanomicelle-based gene delivery into the skeletal muscle. Moreover, the nanomicelle showed significant tumor growth suppression for almost a month by introducing a pDNA expressing a soluble form of vascular endothelial growth factor (VEGF) receptor-1 (sFlt-1) to skeletal muscle to obtain anti-angiogenic effect on tumor growth. This feature of sustained effect gives an important advantage of gene therapy, especially on the points of cost effectiveness and high compliance. These results suggest that the hydrodynamic gene introduction to skeletal muscle using polyplex nanomicelle system possesses the potential for effective gene therapy.

1. Introduction

Skeletal muscle is an interesting target for gene therapy. Not only for the direct treatment of the diseases in the muscle such as muscular dystrophy, gene delivery may use the muscle as a protein factory expressing transgene constitutively [1,2]. This technique has applications to the treatment of peripheral ischemia [3], haematological disorder [4–7] and diabetes mellitus [8,9], as well as for the purpose of DNA vaccination [10] and tissue engineering [11]. Various functional proteins, such as growth factor, have been reported to show therapeutic effects. Muscle-targeting gene delivery was pioneered in 1990 by a simple intra-muscular (i.m.) injection of naked pDNA [12]. Due to the low efficiency of this approach, the research focus was quickly shifted to the application of viral vectors. For the past decade, the majority of animal experiments and clinical trials targeting skeletal muscle have used viral vectors. However, this approach has several serious problems, including the size limitation of contained gene, difficulty of procedures for the manufacture of virus, and especially the immunogenicity derived from the nature of viruses [2].

To solve these issues, non-viral gene carriers have been actively investigated. For muscle targeting, however, most of the gene carriers such as lipoplexes and polyplexes have only given disappointing results, showing a lower transgene expression efficiency than even the naked pDNA. The reasons for this lowered efficiency are not fully understood but it is speculated that the cationic lipoplexes or polyplexes are apt to bind to the negatively charged extracellular matrix (ECM), a basement membrane rich in glycosaminoglycans, in the skeletal muscle [13–15]. Unlike the cells in organs such as the liver, the muscle fibers are surrounded by a layer of mechanically strong ECM, supposedly prohibiting the entry of cationic gene carriers.

On the other hand, a new strategy of targeting skeletal muscle, vascular approach, has attracted much attention [16–18]. This strategy is reasonable from the anatomical characteristics of muscle, because the muscle has an abundant blood vascular supply with extensive capillary network wrapping around the muscle fibers, leading to easier access and direct conduit compared to i.m. injection. Especially, intravenous (i.v.) injection has more benefits than intra-arterial (i.a.) route, due to the easier access under the skin with fewer potential deleterious consequences relating to vessel damage after injection. Wolff et al. reported the i.v. injection of naked pDNA with

* Corresponding author. Department of Materials Engineering, Graduate School of Engineering, The University of Tokyo, 7-3-1 Hongo, Bunkyo-ku, Tokyo 113-0033, Japan. Tel.: +81 3 5841 7138; fax: +81 3 5841 7139.
E-mail address: kataoka@bmw.t.u-tokyo.ac.jp (K. Kataoka).

0168-3659/$ – see front matter © 2009 Elsevier B.V. All rights reserved.
doi:10.1016/j.jconrel.2009.12.014

transient isolation of limb by tourniquet, obtaining higher levels of transgene expression in the skeletal muscle than other methods of i.m. and i.a. injections [18]. The hydrodynamic mechanism of transient increase in the hydrostatic pressure is considered to contribute to the enhanced transgene expression [19]. They had also tried adenovirus vectors by the same injection technique, and interestingly, the naked pDNA showed higher transgene expression than the adenovirus.

Here we describe a new application of gene carrier, polyplex nanomicelle (Fig. 1), to this hydrodynamic gene delivery to skeletal muscle. This system is a polyplex composed of poly(ethyleneglycol) (PEG)-block-polycation and pDNA, forming micelle that has been found suitable for gene delivery: a diameter around 100 nm with a hydrophilic and electrically neutral palisade of PEG, increased tolerance under physiologic conditions with the remarkably low cytotoxicity [20–25]. Due to the stable and biocompatible features, the nanomicelle is expected to achieve the enhanced uptake into the muscle fibers as well as the sustained transgene expression. To our knowledge, the hydrodynamic gene delivery has been investigated mostly using naked pDNA, and there are few non-viral systems to succeed in enhancing the transfection efficiency. Although the naked pDNA delivery has an inherent simplicity, if the higher transgene expression and improved safety are obtained by using a suitable gene carrier, it should be a significant progress for the practical use of hydrodynamic gene delivery to skeletal muscle.

We undertook the present study to investigate the feasibility of the polyplex nanomicelle from PEG-poly(L-lysine) (PEG-PLys)/pDNA for hydrodynamic gene delivery. We performed (1) evaluation of transgene expression over the long term; (2) evaluation of carrier behavior by *in vivo* microscopy analysis; and (3) evaluation of anti-angiogenic effect to inhibit the tumor growth by ectopic expression of vascular endothelial growth factor (VEGF) receptor-1 (sFlt-1) gene in the mice bearing pancreatic adenocarcinoma BxPC3. We demonstrate that the carrier is capable of safely inducing high transgene expression on the targeted muscle, indicating the promising feasibility for therapeutic purposes in the clinical settings.

2. Materials and methods

2.1. Materials

Plasmid DNAs (pDNA) encoding luciferase (pGL4.10: Promega, Madison, WI, USA) and EGFP (pEGFP-C1, 4700 bpa) (Clontech, Palo Alto, CA, USA) were amplified in competent DH5α *Escherichia coli* and purified using a NucleoBond Xtra EF (Nippon Genetics, Tokyo, Japan). pVL 1393 baculovirus vector pDNA encoding human sFlt-1 was kindly provided by Dr. M. Shibuya (Tokyo Medical and Dental University). The pDNA concentration was determined by reading the absorbance at 260 nm. Dulbecco's modified Eagle's medium (DMEM) and fetal bovine serum (FBS) were purchased from Sigma-Aldrich (St. Louis, MO, USA) and Dainippon Sumitomo Pharma Co., Ltd. (Osaka, Japan), respectively. ELISA kits were purchased as below; mouse creatine phosphokinase (CPK): Enzy-Chrom Creatine Kinase Assay kit (ECPK-100) from BioAssay Systems (Hayward, CA, USA), C-reactive protein (CRP): C-Reactive Protein ELISA (971CRP01M-96) from Cosmo Bio Co., Ltd. (Tokyo, Japan), human Soluble VEGF R1/Flt-1 Quantikine Kit (DVR100B) from R&D Systems Inc. (Minneapolis, MN). Rat monoclonal antibody anti-platelet endothelial cell adhesion molecule-1 (PECAM-1), as a marker for vascular ECs, was purchased from BD Pharmingen (Franklin Lakes, NJ). Alexa488-conjugated secondary antibodies to rat IgG were obtained from Invitrogen Molecular Probes (Eugene, OR).

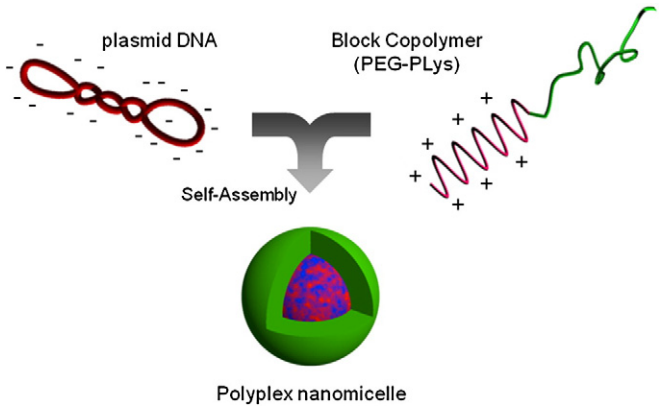

Fig. 1. Polyplex nanomicelle composed of pDNA and block copolymer.

2.2. Animals

Balb/c nude mice (female, 6 weeks old) were purchased from Charles River Laboratories (Tokyo, Japan). The strain of histone–GFP fusion mice (B6.Cg-Tg(HIST1H2BB/EGFP)1 Pa/J) was purchased from the Jackson Laboratory (Bar Harbor, Maine) [26]. All animal experimental protocols were performed in accordance with the Guide for the Care and Use of Laboratory Animals as stated by the National Institutes of Health.

2.3. Synthesis of PEG-PLys block copolymer

A series of poly(ethylene glycol)-poly(L-lysine) (PEG-PLys) block copolymers with different PLys chain length were synthesized as previously reported [23,27]. Briefly, ring opening polymerization of N^{ε}-trifluoroacetyl-L-lysine *N*-carboxyunhydride was initiated by the ω-NH_2 terminal group of α-methoxy-ω-amino PEG ($M_w = 12{,}000$), followed by the removal of trifluoroacetyl protecting groups (TFA) by NaOH. The obtained block copolymer products were confirmed to have a fairly narrow molecular weight distribution ($M_w/M_n = 1.06$–1.10) by gel permeation chromatography (GPC). The degree of polymerization of the PLys segment was determined to be 16, 38, and 88 by comparing ^{1}H NMR integration ratios between methylene protons of PEG chain (CH_2CH_2O) and methylene protons of the side chain of PLys segment ($(CH_2)_3CH_2NH_3$). These block copolymers were termed as PEG-PLys 12–16, 12–38, 12–88, respectively.

2.4. Formation of polyplex nanomicelle

PEG-PLys and pDNA were separately dissolved in 10 mM Tris–HCl buffer adjusted to pH 7.4. Polyplex nanomicelles were obtained by simply mixing both solutions at N/P ratio 2, which is a molar ratio of lysine units in PEG-PLys to nucleotide units in pDNA. The polyplex nanomicelle solution was left for 15 min at room temperature and then subjected to the following experiments. The final pDNA concentration was adjusted to 166.7 mg/ml. Just prior to injection, 1/100 volume of 5 M NaCl solution was added to form half-isotonic solution.

2.5. Hydrodynamic injection into the limb vein of mice

Mice were anesthetized with ketamine/xylazine (80 mg/kg and 5 mg/kg) solution through intraperitoneal injection. Prior to each injection, a tourniquet was placed on the proximal thigh to transiently restrict blood flow. From a distal site of great saphenous vein, the naked pDNA or polyplex nanomicelle solution (300 μl) containing 50 μg pDNA was injected in 5 s. After 5 min of injection, the tourniquet was released.

2.6. Evaluation of luciferase expression

Real-time evaluation of luciferase expression was done by IVIS™ Imaging System (Xenogen, Alameda, CA, US) after intraperitoneal injection of D-luciferin, according to manufacturer's protocol. For the evaluation of transfection efficiency in the muscle tissue, mice were sacrificed and the triceps muscle of calf was extracted with fascia, followed by thorough homogenization using a Multi-beads shocker (Yasui Kikai Corporation, Osaka, Japan). The luciferase expression was measured by a Luciferase Assay System (Promega, Madison, WI, USA) according to the protocol provided by the manufacturer, using a Lumat LB9507 luminometer (Berthold, Bad Wildbad, Germany). The expression was normalized to protein concentrations in cell lysates.

2.7. Evaluation of intact pDNA amount in the muscle

The intact pDNA remaining in the muscle was evaluated by a real-time quantitative PCR using specific primers for Luc2 sequence in the pGL4.10 pDNA: forward primer GGACTTGGACACCGGTAAGA and reverse primer GTCGAAGATGTTGGGGTGTT. From the muscle, the DNA was collected and purified using a Wizard Genomic DNA purification Kit (Promega), then subjected to the PCR using an ABI 7500 Fast Real-Time PCR system (Applied Biosystems, Foster City, CA, USA). This evaluation of remaining pDNA amount was done simultaneously with the luciferase expression measurement by transversely dividing the muscle into two parts, then they were homogenized separately, one for collecting protein and the other for collecting DNA. Normalization of the muscle weight was done by evaluating the copy number of β-actin in the genome DNA from each sample, using TaqMan Gene Expression Assays (Mm00607939 s1 for mouse β-actin). A linear relationship between the muscle weight and threshold cycle for the β-actin gene amplification was confirmed (data not shown).

2.8. Evaluation of TNFα mRNA expression

After injection, the muscle was extracted and the mRNA was collected using RNeasy Fibrous Tissue Kit (Qiagen, Hilden, Germany). The gene expression was analyzed by a real-time quantitative PCR, using TaqMan Gene Expression Assays (Mm00443258 m1 for mouse TNFα).

2.9. In vivo confocal microscopy

A home-built *in vivo* fluorescence confocal laser scanning microscopy system [28] was used to monitor gene expression in individual muscle fibers in mice *in vivo*. Mice were anesthetized by an intraperitoneal injection of ketamine (80 mg/kg) and xylazine (10 mg/kg). Skin incision was carefully made to expose the muscle without damaging fascia. Fluorescence signals of GFP and Cy5 were excited with a 491 nm (Cobalt, Stockholm, Sweden) and a 635 nm continuous-wave laser (Coherent, Santa Clara, CA), respectively and detected through a 520 ± 17 nm and a 670 ± 15 nm band pass filter (Semrock, Rochester, NY), respectively. After each imaging session, the skin incision was closed by 6-0 nylon suture and triple antibiotic ointment was applied.

2.10. Anti-tumor activity assay

Balb/c nude mice were inoculated subcutaneously with BxPC3, a human pancreatic adenocarcinoma cell line (American Type Culture Collection, Manassas, VA) (5×10^6 cells in 100 μl of PBS). Tumors were allowed to grow for 2–3 weeks to reach proliferative phase (the size of tumor at this point was approximately 60 mm^3). After twice hydrodynamic injection of naked pDNA or polyplex nanomicelle (Days 0 and 7), tumor growth were checked twice a week. Tumor volume (V) was calculated as the following equation:

$$V = a \times b^2 / 2$$

where the letters a and b denote the long and short diameters of the tumor tissue. Intergroup differences were tested for significance using Student's t-test. p values less than 0.05 were considered to be significant.

2.11. Evaluation of vascular density

After 10 days of hydrodynamic injection of naked pDNA or polyplex nanomicelle to tumor-bearing mice as described above, mice were sacrificed and the tumors were excised, frozen in dry-iced acetone, and sectioned at 10 μm thickness in a cryostat. Immunostaining was carried out using anti-PECAM-1 antibody followed by Alexa 488-conjugated secondary antibody for immunostaining of vascular ECs. The samples were observed by a confocal laser scanning microscope (CLSM). The CLSM observation was performed using an LSM 510 (Carl Zeiss, Oberlochen, Germany) with an EC Plan-Neoflur 20× objective (Carl Zeiss) at the excitation wavelength of 488 nm (Ar laser). PECAM-1 positive area (%) was calculated from Alexa 488 positive pixels.

3. Results and discussion

3.1. Transgene expression in the skeletal muscle

The hydrodynamic delivery was done by i.v. injection of pDNA or polyplex nanomicelle into the great saphenous vein of the distal hind limb (Fig. 2). Just before the injection, a tourniquet was placed on the proximal thigh, and kept during the injection and for 5 min postinjection. Three hundred μl solution containing 50 μg pDNA was injected. Slight swelling was observed on the limb after injection but disappeared within an hour, and no obvious functional loss on the leg had been observed since then.

The transgene expression was evaluated by IVIS™ Imaging System (Xenogen, Alameda, CA, US) using a luciferase-expressing pDNA. This method is advantageous as the expression on the identical mice can be followed continuously. Fig. 3A shows the representative images on Day 6 after transgene introduction. The luciferase expression was visualized on the area of lower thigh regardless to the gene carriers, and by a separate experiment to analyze the tissue samples such as muscle, skin, bone and tendinous tissue, the triceps muscle of the calf was revealed to be the chief target expressing luciferase in the injected limb (data not shown). We did imaging approximately every

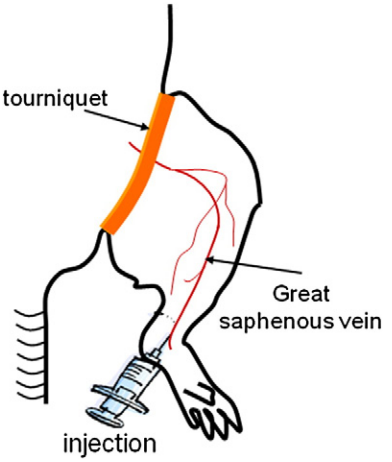

Fig. 2. Schematic representation of hydrodynamic gene delivery to skeletal muscle. pDNA or polyplex nanomicelle was intravenously injected with isolation of the limb.

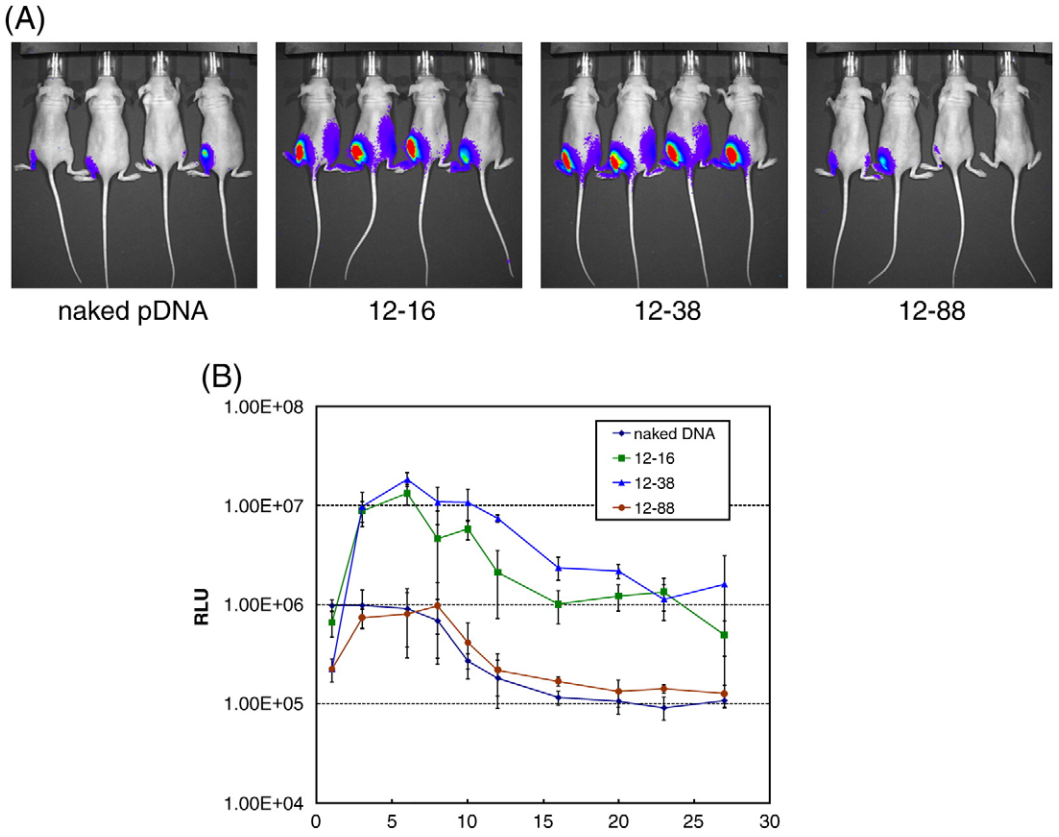

Fig. 3. Luciferase expression on skeletal muscle after injection of pDNA or polyplex nanomicelles. (A) IVIS images of mice after 6 days of injection. (B) Time-dependent profiles of luciferase expression quantified from IVIS images ($n=4$, ± SEM).

3 days and calculated the amount of luciferase expression from the image of each mouse. As shown in Fig. 3B, the polyplex nanomicelles of 12–16 and 12–38 showed tenfold higher expression than naked pDNA and 12–88 after Day 3. The time-dependent profiles of expression, reaching the peak around Day 6 and the subsequent gradual decrease, were similar among the carriers. Notably, the expression was still clearly detectable in the nanomicelles of 12–16 and 12–38 on Day 27.

The expression from naked pDNA was higher than the nanomicelles on Day 1. By the evaluation of luciferase expression from the extracted samples of the muscle, the higher expression by naked pDNA was also confirmed compared to 12–38 nanomicelles on Day 1 (Table 1). However, by Day 5, the naked pDNA and the nanomicelle showed remarkably different profiles; the latter exhibited tenfold increase in the expression while the former showed slight decrease, and eventually the latter showed higher expression than the former on Day 5. This trend was well correlated with the amount of intact pDNA remaining in the muscle evaluated by real-time quantitative PCR. For the animals dosed with naked pDNA, the intact pDNA remaining in the muscle was estimated to 2.4 ng/mg muscle on Day 1, which corresponded to only 0.1% of the injected dose, providing the muscle on the lower thigh to have 20 mg weight. Then on Day 5, the amount of pDNA showed a significant decrease to a hundredth part to that on Day 1. In contrast, using the nanomicelle, the intact pDNA amount was two-digit higher (457.3 ng/mg muscle 10% of the injected dose) than that observed by the naked pDNA injection on Day 1, and showed only a moderate decrease to one-tenth on Day 5.

Table 1
Luciferase expression and pDNA uptake evaluated from extracted muscle ($n=3$).

	Luciferase expression (RLU/mg protein)		Intact pDNA amount (ng/mg muscle)	
	Day 1	Day 5	Day 1	Day 5
Naked pDNA	331209.7	102510.5	2.4	0.03
Nanomicelle	75859.8	867026.6	457.3	14.53
Control	200.5	102.0	Undetected	Undetected

The hydrodynamic pressure is known to facilitate the internalization of the injected pDNA directly into cells in the tissue, and eventually, even naked pDNA induces substantial transgene expression [19,29–31]. The naked pDNA may induce the rapid transcription if it is safely transferred into the cells. In this regard, it is reasonable that the naked pDNA showed higher transgene expression than polyplex nanomicelle on Day 1 in this study. However, in this case, the naked pDNA was rapidly degraded as seen in Table 1, resulting in the rapid decrease in the expression. In contrast, polyplex nanomicelle may contribute to the increased stability of the loaded pDNA in the physiological condition, leading to the gradual increase in transgene expression for a week, eventually to the level of one-digit higher than that of the naked pDNA. It is interesting to note that the chain length of PLys in PEG-PLys block copolymer significantly affected the capacity of transgene expression. We previously reported that the extended chain length of PLys provided the increased tolerability of the loaded pDNA toward nuclease and the improved stability in the presence of serum of the polyplex nanomicelle, leading to the higher transfection toward cultured cells in serum-containing medium [21,23]. However, in this study, the opposite trend was apparently observed in *in vivo* expression toward the muscle cells by hydrodynamic injection. Extension of PLys segment length in the nanomicelles resulted in the lowered expression as typically seen in Fig. 3. Presumably, as cellular internalization is not the major limiting step in hydrodynamic transfection, the controlled unpackaging of the loaded pDNA from the nanomicelles in intracellular environment may be a key step for a substantially high and sustained transgene expression. Nanomicelles with shorter PLys chain (12–16 and 12–38)

are less stable than those with longer PLys chain (12–88), thereby smoothly release the loaded pDNA inside of muscle cells to exert higher transgene expression without the problem of overstabilization. Hereafter, we used the nanomicelle from the 12–38 block copolymer in the experiments because of its substantially high *in vivo* transfection capacity.

3.2. Evaluation by in vivo confocal microscopy

For dynamic evaluation in the muscle tissues, we observed the muscle fibers after hydrodynamic injection of EGFP-expressing pDNA as a form of naked pDNA or polyplex nanomicelle (12–38), using a video-rate confocal imaging system developed for real-time *in vivo* imaging. The muscle was excited from the surface of fascia and the confocal images were obtained sequentially at every 10 μm thickness. Fig. 4 represents the typical images obtained at the depth between 20 and 40 μm from the surface on Day 6. The EGFP-positive fibers were observed among the aligned muscle fibers. In naked pDNA, a small number of EGFP-positive fibers were found, surrounded by a larger number of EGFP-negative fibers. In contrast, there was observed an increased number of EGFP-positive fibers for the sample transfected with the nanomicelles. In both cases, no apparent damage on the fibers was observed compared to the control limb without injection.

Then, to investigate the retention of pDNA in the muscle tissue, Cy5-labeled pDNA was applied to histone–GFP mice, in which every cell stably expressed GFP signal in the nuclei. Plasmid DNA was labeled using a Label IT nucleic acid labeling kit (Panvera, Madison, WI, USA), that promotes covalent attachment of specific fluorescent molecules to guanine residues in DNA. The labeled pDNA, observed as red spots, was widely distributed in the muscle tissue for both naked pDNA and polyplex nanomicelle on Day 1 (Fig. 5A). On Day 3 and Day 7, the total number of red spots in the tissue was apparently decreased compared to Day 1. To evaluate the time-dependent change quantitatively, we analyzed the images using an image analysis software (In Cell Analyzer 1000 Workstation ver.3.5, GE Healthcare UK Ltd. Buckinghamshire, England), where each nucleus was recognized one by one, and the ratio of nuclei co-localizing with red spots was calculated for more than 500 nuclei at each time point. Interestingly, in contrast to the naked pDNA that showed significant decrease in the ratio of co-localization at Day 3, the nanomicelle kept an appreciably high co-localization ratio until Day 3, then turned to a gradual decrease (Fig. 5B). This result demonstrates that pDNA loaded in the nanomicelle stably remained in the cells, leading to the sustained transgene expression. This observation is well consistent with the results of time-dependent profile of transgene expression (Fig. 3B) and the quantification of intact pDNA in the tissue (Table 1), highlighting the feature of the polyplex nanomicelles relevant for hydrodynamic gene delivery system.

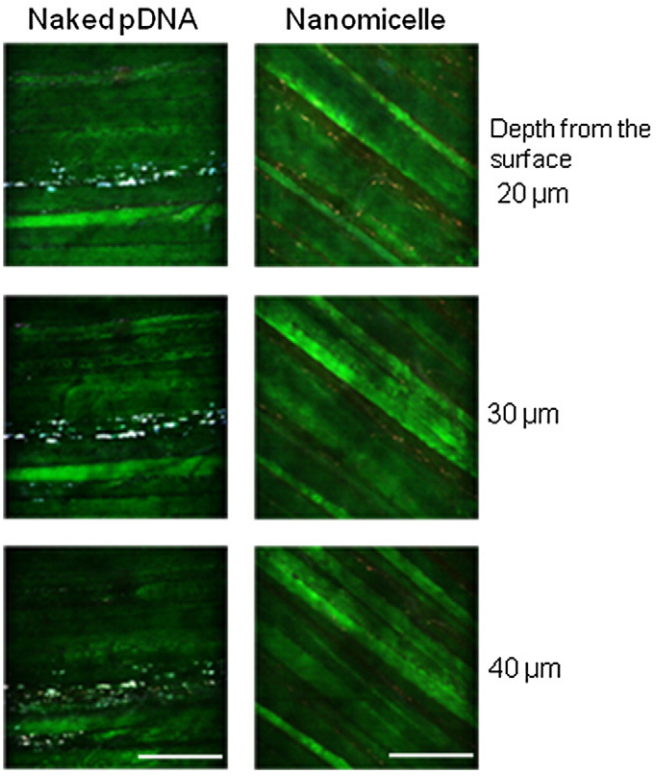

Fig. 4. EGFP expression on skeletal muscle on Day 6 after injection of naked pDNA or polyplex nanomicelle (12–38). Confocal images were obtained using an *in vivo* fluorescence confocal laser scanning microscopy system by excitation from the surface of fascia. The value on the right of each image indicates the depth from the surface. Bars represent 100 μm.

3.3. Evaluation of safety issues

The transient enhancement in the permeability of plasma membrane is considered to be a major mechanism of gene introduction by hydrodynamic method [19]. In turn, this may induce the transient leakage of cytoplasmic components into the exterior. Indeed, the hydrodynamic injection to liver transiently elevated alanine aminotransferase and aspartate aminotransferase level in serum [31]. However, no apparent damage was histologically found in the liver without any functional disorder. Creatine phosphokinase (CPK) elevation in serum was reported for hydrodynamic gene transfer into skeletal muscle, yet the elevation was only transient [18].

Consistent with these literatures, the injection of polyplex nanomicelle induced elevation of CPK on Day 1 as well as naked pDNA, but on Day 6 the value recovered to the control level. No significant difference was observed between naked pDNA and nanomicelle (Table 2). C-reactive protein (CRP), a sensitive marker protein for inflammation, was not detected by both naked pDNA and nanomicelles after hydrodynamic injection.

To further investigate the toxic effect of injection, the induction of an inflammatory cytokine, TNFα, was evaluated. As for the systemic effect, no TNFα protein was detected in serum by an ELISA assay after one day from the hydrodynamic injection (data not shown). However, when the TNFα mRNA expression in the muscle tissue was evaluated using a quantitative PCR, the naked pDNA induced three-fold increase in the expression compared to non-treated control (Fig. 6). Instead, the nanomicelle showed almost no change in the TNFα mRNA expression. Although the mechanism of TNFα induction by naked pDNA is unclear, it is reasonable that almost no cytokine induction was detected by nanomicelle injection because of the reduced foreign-body recognition presumably due to the PEG palisade as previously described. Accordingly, these results support the safety of nanomicelle-based gene delivery into the skeletal muscle.

3.4. Tumor growth inhibition by ectopic introduction of sFlt-1 gene

Finally, we evaluated the therapeutic feasibility of muscle-targeting gene delivery using nanomicelle. For this purpose, a pDNA expressing a soluble form of vascular endothelial growth factor (VEGF) receptor-1 (sFlt-1) was used to obtain anti-angiogenic effect on tumor growth [32]. This strategy of gene therapy has already attracted much attention, utilizing anti-angiogenesis to inhibit growth of new blood vessels around the solid tumor [33–37]. The skeletal muscle is one of the promising targets for the gene delivery to expect the long-term secretion of sFlt-1, and such delivery methods as i.m. injection of adnovirus [38], adeno-associated virus [39], and i.m. injection of naked pDNA followed by electroporation [40] had been

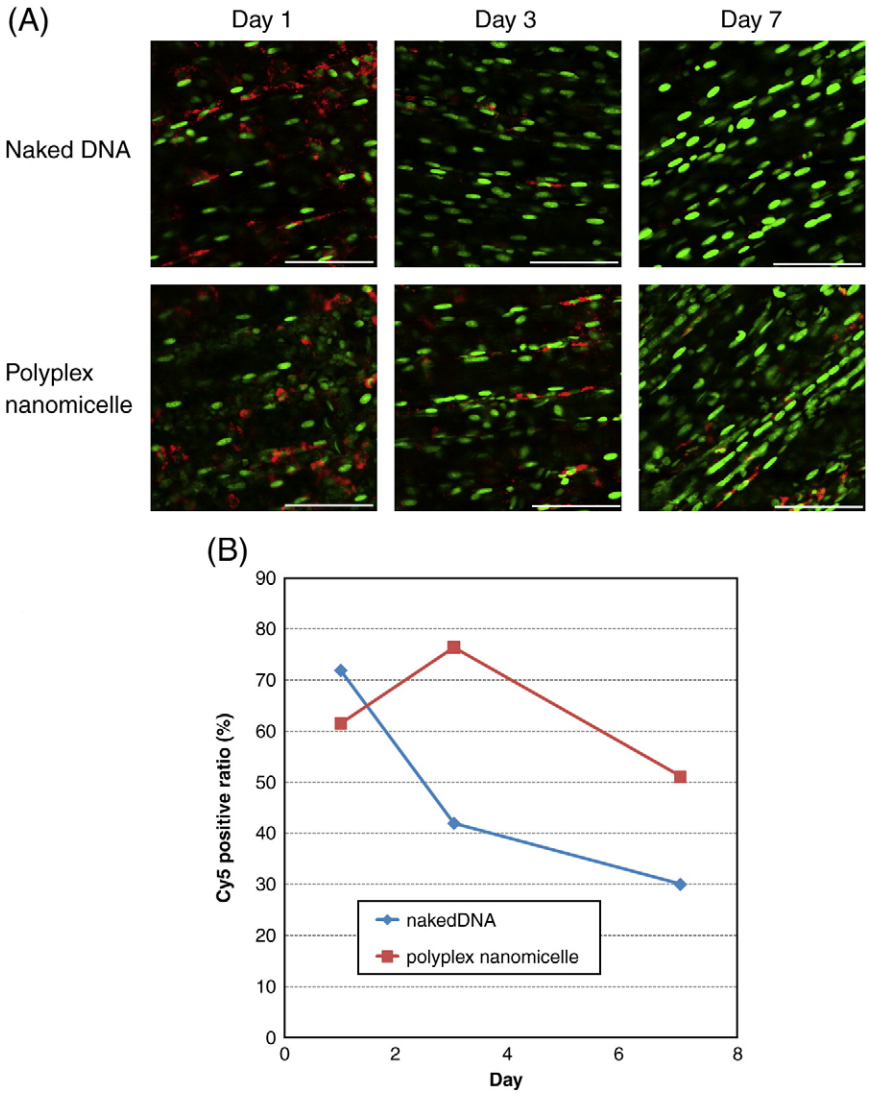

Fig. 5. Distribution of Cy5-labeled pDNA in the muscle fibers after hydrodynamic injection of naked pDNA or polyplex nanomicelle (12–38). (A) Confocal images of Cy5-labeled pDNA in histone-GFP mice, in which every cell stably expresses GFP signal in the nuclei. Bars represent 100 μm. (B) Evaluation of co-localization ratios of nuclei and pDNA using an image analysis software (In Cell Analyzer 1000 Workstation ver.3.5, GE Healthcare UK Ltd).

tried to obtain anti-angiogenic effect. Thus, we applied the hydrodynamic injection using the nanomicelle to deliver sFlt-1 effectively to skeletal muscle.

The hydrodynamic injection of naked pDNA encoding sFlt-1 or polyplex nanomicelle was done twice with one-week interval to mice bearing pancreatic adenocarcinoma BxPC3, followed by the measurement of tumor volume for a month. As shown in Fig. 7A, the tumor growth was significantly suppressed using the sFlt-1-expressing pDNA. Both naked pDNA and nanomicelle showed equivalent effect of tumor growth inhibition for more than two weeks postinjection. The sFlt-1 protein in serum was similarly detected in both methods on Day 10 by an ELISA assay (Fig. 7B), consistent with the equivalent inhibition of tumor growth. Moreover, to confirm that the tumor growth suppression was attributed to the anti-angiogenic effect, the vascular density was evaluated in the tumor using a monoclonal antibody anti-platelet endothelial cell adhesion molecule-1 (PECAM-1), as a marker for

Table 2
Serum concentration of creatine phosphokinase (CPK) after hydrodynamic injection of naked pDNA or polyplex nanomicelles ($n=4$).

CPK (U/L)	Control	Naked pDNA	PEG-PLys (12–16)	PEG-PLys (12–38)
Day 1	62.7	113.3	86.8	163.1
Day 6		68.8	59.4	57.8

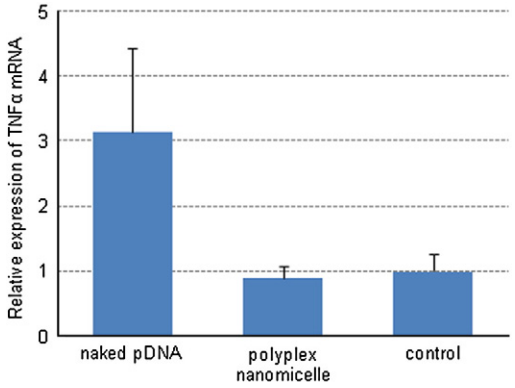

Fig. 6. Evaluation of TNFα induction after hydrodynamic injection of naked pDNA or polyplex nanomicelle (12–38). TNFα mRNA expression in the muscle tissue was evaluated by a quantitative PCR, and presented as a relative value to non-treated control ($n=3$, ± SEM).

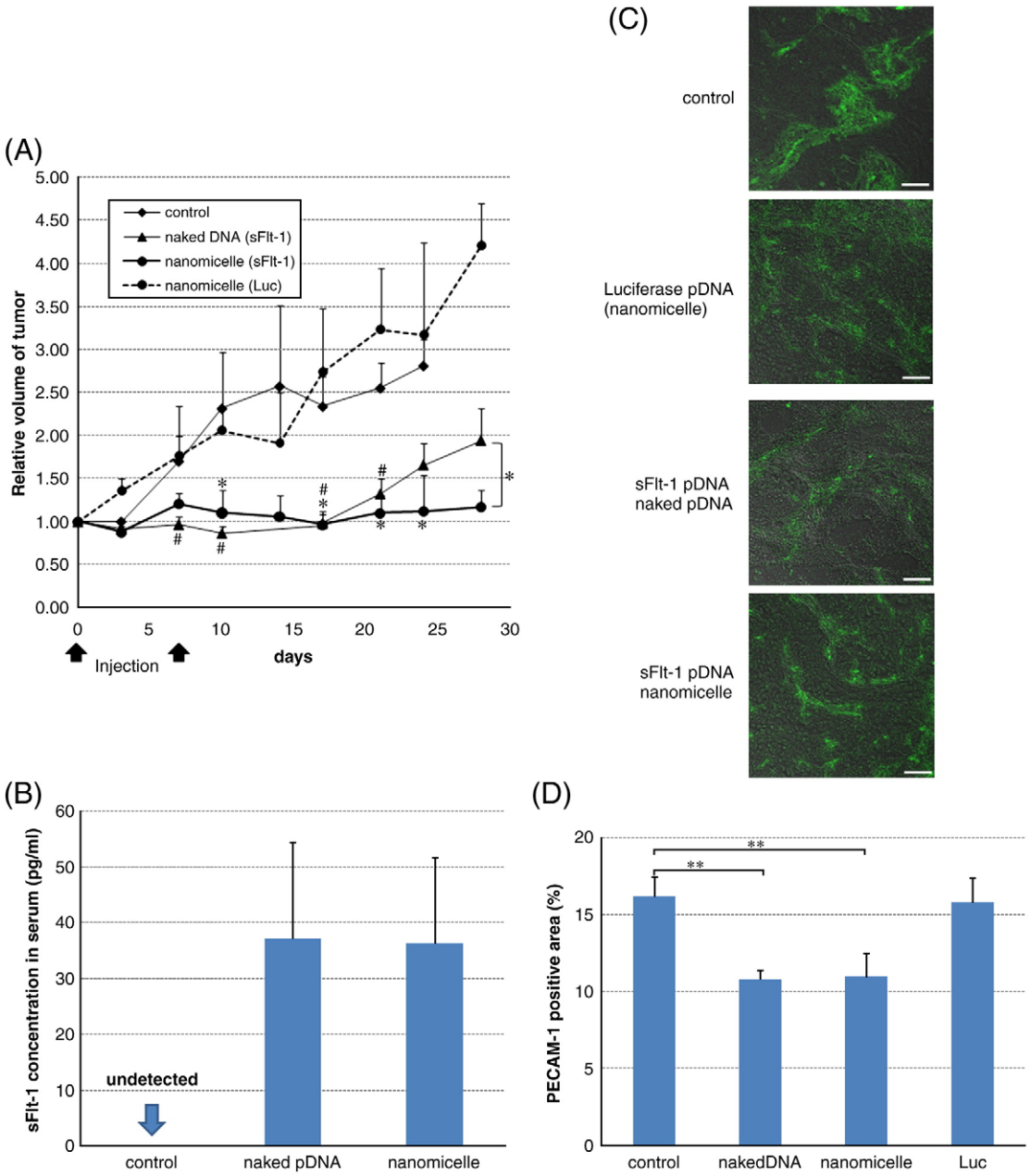

Fig. 7. Evaluation of anti-angiogenic effect on tumor growth by ectopic introduction of sFlt-1 gene into skeletal muscle after hydrodynamic injection. (A) Tumor growth inhibition after injection. Naked pDNA or polyplex nanomicelle (12–38) was injected twice with one-week interval to mice bearing pancreatic adenocarinoma BxPC3. The tumor volume was shown as a relative value to that on Day 0 ($n=4$, ± SEM). *$p<0.05$ for nanomicelle (sFlt-1) versus control (except Day 28). *$p<0.05$ for nanomicelle (sFlt-1) versus naked pDNA (Day 28). #$p<0.05$ for naked pDNA (sFlt-1) versus control. (B) sFlt-1 concentration in serum evaluated by an ELISA assay on Day 10 after injection ($n=4$, ± SEM). (C) Confocal images of tumor tissue on Day 10. To evaluate the anti-angiogenic effect, the tumor tissue was treated with a monoclonal antibody anti-platelet endothelial cell adhesion molecule-1 (PECAM-1) to show the vascular density. Bars represent 10 μm. (D) PECAM-1 positive areas calculated from the images. The ratios of PECAM-1 positive endothelium area per total area were presented ($n=4$, ± SEM).

vascular endothelial cells (Fig. 7C). From these images, the ratios of PECAM-1 positive endothelium area per the total area were calculated. As shown in Fig. 7D, it was revealed that the areas of PECAM-1 positive were lower in the mice treated by the sFlt-1 pDNA than that of control mice. Thus, it is confirmed that the ectopic expression of sFlt-1 provided therapeutic outcome of tumor growth inhibition by anti-angiogenic effect.

To be mentioned is that polyplex nanomicelle showed the prolonged effect on tumor growth inhibition for more than three weeks after the initial injection. On Day 28, the nanomicelle showed significant suppression on tumor growth compared with naked pDNA. It is likely to be attributed to the sustained transgene expression by nanomicelle as shown in Fig. 3 and Table 1. This feature of sustained effect gives an important advantage of gene therapy over other molecular-targeting drugs, such as bevacizumab (Avastin) for anti-angiogenesis treatment, on the points of cost effectiveness and high compliance. Although much further investigation is needed to clarify the therapeutic effect, the polyplex nanomicelle is considered to be a good candidate as a carrier to realize clinical gene therapy.

In conclusion, we evaluated the polyplex nanomicelle composed of pDNA and PEG-PLys block copolymer for hydrodynamic gene delivery to skeletal muscle. Due to the high stability and biocompatibility, the nanomicelle provided excellent and prolonged transgene expression in the muscle compared to naked pDNA. As far as we know, this

system is the first non-viral system to show effective transgene expression by hydrodynamic gene delivery, appealing its promise for clinical application.

Acknowledgements

This work was financially supported in part by Grants-in-Aid for Scientific Research from the Japanese Ministry of Education, Culture, Sports, Science and Technology, Japan (K. I.), Medical Research Grant on Traffic Accident from the General Insurance Association of Japan (K. I.), and the Core Research Program for Evolutional Science and Technology (CREST) from Japan Science and Technology Corporation (JST) (K. K.). We thank Dr. Masabumi Shibuya (Tokyo Medical and Dental University) for providing pVL 1393 baculovirus vector pDNA encoding human sFlt-1. We appreciate Ms. Noriko Oshima (GE Healthcare Bio-Sciences KK) for technical support of operating the image analysis software. We also appreciate Dr. Makoto Oba, Dr. Yu Matsumoto and Ms. Yoko Hasegawa (The University of Tokyo) for technical assistance.

References

[1] H.M. Blau, M.L. Springer, Muscle-mediated gene therapy, N. Engl. J. Med. 333 (1995) 1554–1556.
[2] Q.L. Lu, G. Bou-Gharios, T.A. Partridge, Non-viral gene delivery in skeletal muscle: a protein factory, Gene Ther. 10 (2003) 131–142.
[3] I. Baumgartner, J.M. Isner, Stimulation of peripheral angiogenesis by vascular endothelial growth factor (VEGF), Vasa 27 (1998) 201–206.
[4] G. Rizzuto, M. Cappelletti, D. Maione, R. Savino, D. Lazzaro, P. Costa, I. Mathiesen, R. Cortese, G. Ciliberto, R. Laufer, N. La Monica, E. Fattori, Efficient and regulated erythropoietin production by naked DNA injection and muscle electroporation, Proc. Natl. Acad. Sci. U. S. A. 96 (1999) 6417–6422.
[5] P. Kreiss, M. Bettan, J. Crouzet, D. Scherman, Erythropoietin secretion and physiological effect in mouse after intramuscular plasmid DNA electrotransfer, J. Gene Med. 1 (1999) 245–250.
[6] E. Fattori, M. Cappelletti, I. Zampaglione, C. Mennuni, F. Calvaruso, M. Arcuri, G. Rizzuto, P. Costa, G. Perretta, G. Ciliberto, N. La Monica, Gene electro-transfer of an improved erythropoietin plasmid in mice and non-human primates, J. Gene Med. 7 (2005) 228–236.
[7] M.G. Sebestyen, J.O. Hegge, M.A. Noble, D.L. Lewis, H. Herweijer, J.A. Wolff, Progress toward a nonviral gene therapy protocol for the treatment of anemia, Hum. Gene Ther. 18 (2007) 269–285.
[8] T. Murakami, M. Arai, Y. Sunada, A. Nakamura, VEGF 164 gene transfer by electroporation improves diabetic sensory neuropathy in mice, J. Gene Med. 8 (2006) 773–781.
[9] G.J. Prud'homme, R. Draghia-Akli, Q. Wang, Plasmid-based gene therapy of diabetes mellitus, Gene Ther. 14 (2007) 553–564.
[10] G.J. Prud'homme, Y. Glinka, A.S. Khan, R. Draghia-Akli, Electroporation-enhanced nonviral gene transfer for the prevention or treatment of immunological, endocrine and neoplastic diseases, Curr. Gene Ther. 6 (2006) 243–273.
[11] M.D. Kofron, C.T. Laurencin, Bone tissue engineering by gene delivery, Adv. Drug Deliv. Rev. 58 (2006) 555–576.
[12] J.A. Wolff, R.W. Malone, P. Williams, W. Chong, G. Acsadi, A. Jani, P.L. Felgner, Direct gene transfer into mouse muscle in vivo, Science 247 (1990) 1465–1468.
[13] M. Ruponen, S. Ronkko, P. Honkakoski, J. Pelkonen, M. Tammi, A. Urtti, Extracellular glycosaminoglycans modify cellular trafficking of lipoplexes and polyplexes, J. Biol. Chem. 276 (2001) 33875–33880.
[14] N.J. Caron, Y. Torrente, G. Camirand, M. Bujold, P. Chapdelaine, K. Leriche, N. Bresolin, J.P. Tremblay, Intracellular delivery of a Tat-eGFP fusion protein into muscle cells, Mol. Ther. 3 (2001) 310–318.
[15] M. Ruponen, P. Honkakoski, S. Ronkko, J. Pelkonen, M. Tammi, A. Urtti, Extracellular and intracellular barriers in non-viral gene delivery, J. Control. Release 93 (2003) 213–217.
[16] V. Budker, G. Zhang, I. Danko, P. Williams, J. Wolff, The efficient expression of intravascularly delivered DNA in rat muscle, Gene Ther. 5 (1998) 272–276.
[17] G. Zhang, V. Budker, P. Williams, V. Subbotin, J.A. Wolff, Efficient expression of naked dna delivered intraarterially to limb muscles of nonhuman primates, Hum. Gene Ther. 12 (2001) 427–438.
[18] J.E. Hagstrom, J. Hegge, G. Zhang, M. Noble, V. Budker, D.L. Lewis, H. Herweijer, J.A. Wolff, A facile nonviral method for delivering genes and siRNAs to skeletal muscle of mammalian limbs, Mol. Ther. 10 (2004) 386–398.
[19] H. Herweijer, J.A. Wolff, Gene therapy progress and prospects: hydrodynamic gene delivery, Gene Ther. 14 (2007) 99–107.
[20] S. Katayose, K. Kataoka, Water-soluble polyion complex associates of DNA and poly(ethylene glycol)-poly(L-lysine) block copolymer, Bioconjug. Chem. 8 (1997) 702–707.
[21] S. Katayose, K. Kataoka, Remarkable increase in nuclease resistance of plasmid DNA through supramolecular assembly with poly(ethylene glycol)-poly(L-lysine) block copolymer, J. Pharm. Sci. 87 (1998) 160–163.
[22] K. Kataoka, A. Harada, Y. Nagasaki, Block copolymer micelles for drug delivery: design, characterization and biological significance, Adv. Drug Deliv. Rev. 47 (2001) 113–131.
[23] K. Itaka, K. Yamauchi, A. Harada, K. Nakamura, H. Kawaguchi, K. Kataoka, Polyion complex micelles from plasmid DNA and poly(ethylene glycol)-poly(L-lysine) block copolymer as serum-tolerable polyplex system: physicochemical properties of micelles relevant to gene transfection efficiency, Biomaterials 24 (2003) 4495–4506.
[24] K. Osada, K. Kataoka, Drug and gene delivery based on supramolecular assembly of PEG-polypeptide hybrid block copolymers, Adv. Polym. Sci. 202 (2006) 113–153.
[25] K. Itaka, K. Kataoka, Recent development of nonviral gene delivery systems with virus-like structures and mechanisms, Eur. J. Pharm. Biopharm. 71 (2009) 475–483.
[26] A.K. Hadjantonakis, V.E. Papaioannou, Dynamic in vivo imaging and cell tracking using a histone fluorescent protein fusion in mice, BMC Biotechnol. 4 (2004) 33.
[27] A. Harada, K. Kataoka, Formation of polyion complex micelles in an aqueous milieu from a pair of oppositely-charged block copolymers with poly(ethylene glycol) segments, Macromolecules 28 (1995) 5294–5299.
[28] P. Kim, M. Puoris'haag, D. Cote, C.P. Lin, S.H. Yun, In vivo confocal and multiphoton microendoscopy, J. Biomed. Opt. 13 (2008) 010501.
[29] F. Liu, Y. Song, D. Liu, Hydrodynamics-based transfection in animals by systemic administration of plasmid DNA, Gene Ther. 6 (1999) 1258–1266.
[30] G. Zhang, V. Budker, J.A. Wolff, High levels of foreign gene expression in hepatocytes after tail vein injections of naked plasmid DNA, Hum. Gene Ther. 10 (1999) 1735–1737.
[31] N. Kobayashi, M. Nishikawa, K. Hirata, Y. Takakura, Hydrodynamics-based procedure involves transient hyperpermeability in the hepatic cellular membrane: implication of a nonspecific process in efficient intracellular gene delivery, J. Gene Med. 6 (2004) 584–592.
[32] M. Shibuya, S. Yamaguchi, A. Yamane, T. Ikeda, A. Tojo, H. Matsushime, M. Sato, Nucleotide sequence and expression of a novel human receptor-type tyrosine kinase gene (flt) closely related to the fms family, Oncogene 5 (1990) 519–524.
[33] R.L. Kendall, K.A. Thomas, Inhibition of vascular endothelial cell growth factor activity by an endogenously encoded soluble receptor, Proc. Natl. Acad. Sci. U. S. A. 90 (1993) 10705–10709.
[34] K.A. Thomas, Vascular endothelial growth factor, a potent and selective angiogenic agent, J. Biol. Chem. 271 (1996) 603–606.
[35] R.L. Kendall, G. Wang, K.A. Thomas, Identification of a natural soluble form of the vascular endothelial growth factor receptor, FLT-1, and its heterodimerization with KDR, Biochem. Biophys. Res. Commun. 226 (1996) 324–328.
[36] H.L. Kong, D. Hecht, W. Song, I. Kovesdi, N.R. Hackett, A. Yayon, R.G. Crystal, Regional suppression of tumor growth by in vivo transfer of a cDNA encoding a secreted form of the extracellular domain of the flt-1 vascular endothelial growth factor receptor, Hum. Gene Ther. 9 (1998) 823–833.
[37] W.J. Kim, J.W. Yockman, M. Lee, J.H. Jeong, Y.H. Kim, S.W. Kim, Soluble Flt-1 gene delivery using PEI-g-PEG-RGD conjugate for anti-angiogenesis, J. Control. Release 106 (2005) 224–234.
[38] K. Takayama, H. Ueno, Y. Nakanishi, T. Sakamoto, K. Inoue, K. Shimizu, H. Oohashi, N. Hara, Suppression of tumor angiogenesis and growth by gene transfer of a soluble form of vascular endothelial growth factor receptor into a remote organ, Cancer Res. 60 (2000) 2169–2177.
[39] Y. Takei, H. Mizukami, Y. Saga, I. Yoshimura, Y. Hasumi, T. Takayama, T. Kohno, T. Matsushita, T. Okada, A. Kume, M. Suzuki, K. Ozawa, Suppression of ovarian cancer by muscle-mediated expression of soluble VEGFR-1/Flt-1 using adeno-associated virus serotype 1-derived vector, Int. J. Cancer 120 (2007) 278–284.
[40] N. Hamada, K. Kuwano, M. Yamada, N. Hagimoto, K. Hiasa, K. Egashira, N. Nakashima, T. Maeyama, M. Yoshimi, Y. Nakanishi, Anti-vascular endothelial growth factor gene therapy attenuates lung injury and fibrosis in mice, J. Immunol. 175 (2005) 1224–1231.